

Cell Reports, Volume 34

Supplemental information

**Cell-type-specific recruitment of GABAergic
interneurons in the primary somatosensory
cortex by long-range inputs**

Shovan Naskar, Jia Qi, Francisco Pereira, Charles R. Gerfen, and Soohyun Lee

SUPPLEMENTAL INFORMATION

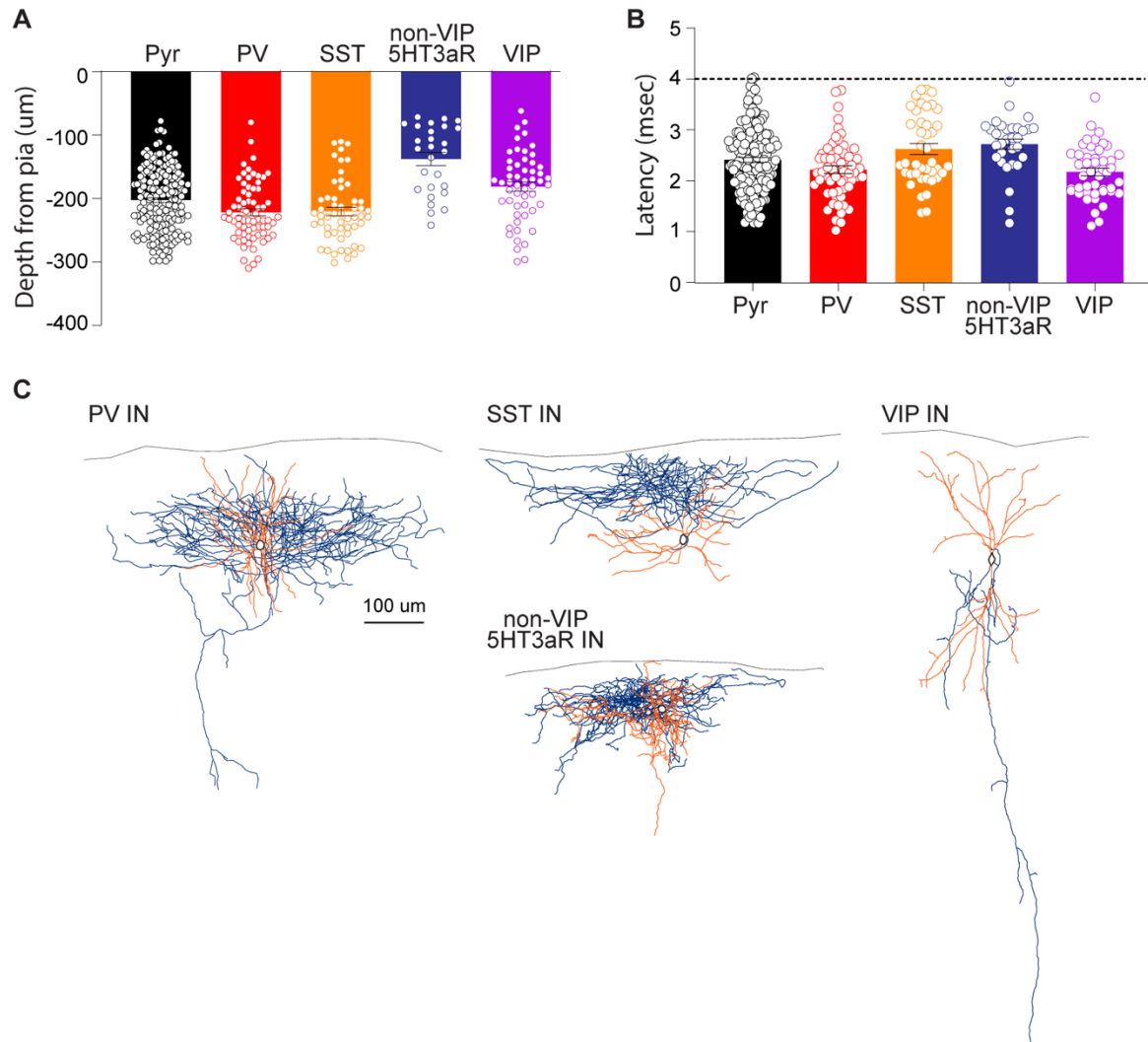


Figure S1. Recording depth, latency of photostimulation-evoked response, and morphology of different groups of neurons in S1. Related to Figure 2. (A) Recording depth (µm) was measured from pia (Pyr cells, 214.32 ± 4.1 , $n = 197$, 96 mice; PV INs, 232.19 ± 6.4 , $n = 70$, 26 mice; SST INs, 246.13 ± 9.5 , $n = 58$, 28 mice; VIP INs, 189.68 ± 8.89 , $n = 60$, 25 mice; nonVIP-5HT3aR INs, 119.08 ± 8.24 , $n = 33$, 17 mice). **(B)** Photostimulation-evoked latency (msec) was measured from the onset of the photostimulation (Pyr cells, 2.43 ± 0.05 , $n = 197$, 96 mice; PV INs, 2.22 ± 0.07 , $n = 70$, 26 mice; SST INs, 2.75 ± 0.13 , $n = 58$, 28 mice; nonVIP-5HT3aR INs, 2.83 ± 0.13 , $n = 33$, 17 mice; VIP INs, 2.18 ± 0.07 , $n = 60$, 25 mice). **(C)** Examples of morphological reconstructions of 4 different types of GABAergic INs using Neurolucida tracing. Orange indicates dendrites and blue indicates axons.

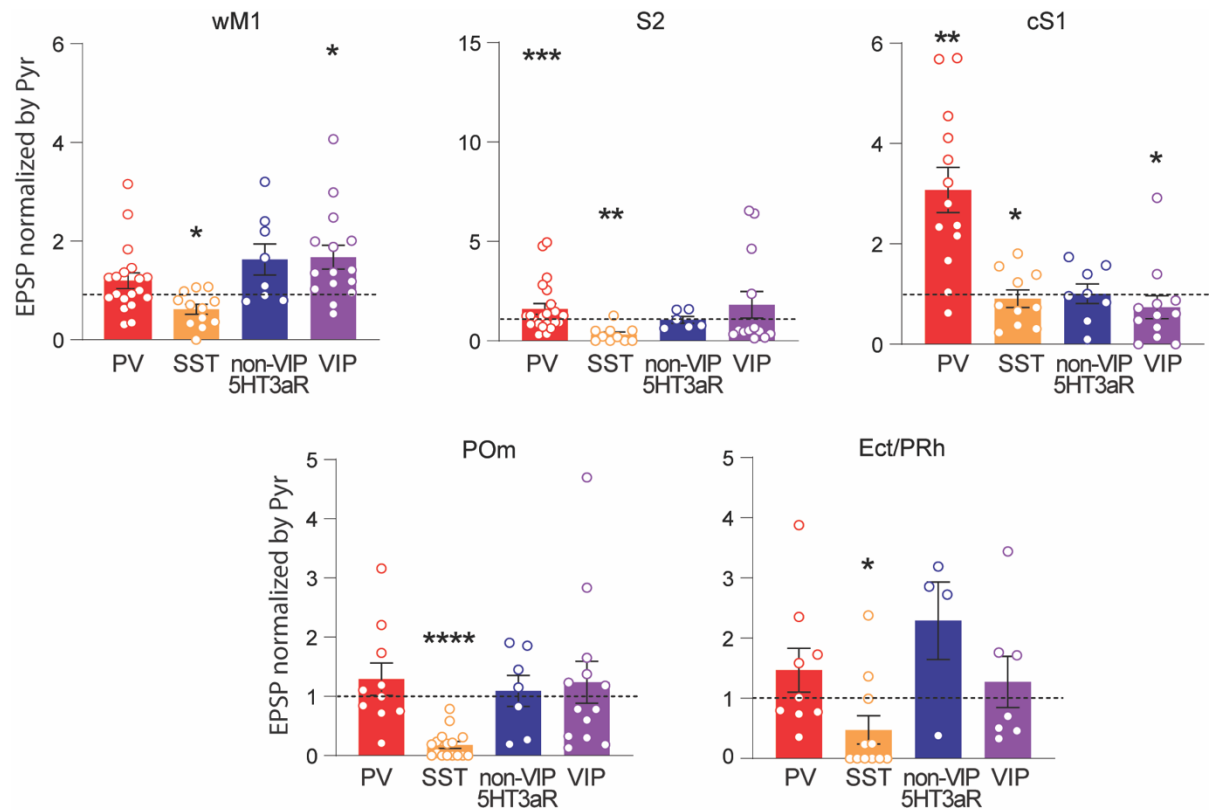


Figure S2. Long-range excitatory inputs from diverse brain areas to different types of GABAergic neurons in the supragranular layers of S1. Related to Figure 2. Photo-stimulation evoked EPSPs from different types of INs were normalized to the EPSPs recorded from nearby pyramidal neurons. Evoked EPSPs were recorded at V_{rest} (Input area, GABAergic INs, mean \pm s.e.m., number of recorded neurons, number of mice used, p value; wM1 input, PV INs, 1.20 ± 0.16 , 19, 6, $p = 0.2253$, SST INs, 0.60 ± 0.10 , 11, 3, $*p = 0.0161$, nonVIP-5HT3aR INs, 1.62 ± 0.31 , 8, 3, $p = 0.5469$, VIP INs, 1.67 ± 0.24 , 15, 7, $*p = 0.0215$; S2 input, PV INs, 3.77 ± 0.71 , 15, 6, $***p = 0.0003$, SST INs, 0.32 ± 0.12 , 10, 5, $**p = 0.0039$, nonVIP-5HT3aR INs, 1.05 ± 0.17 , 6, 2, $p = 0.6875$, VIP INs, 1.81 ± 0.66 , 13, 5, $p = 0.1909$; cS1 input, PV INs, 3.07 ± 0.44 , 13, 5, $**p = 0.0012$, SST INs, 0.90 ± 0.17 , 10, 6, $*p = 0.0322$, nonVIP-5HT3aR INs, 1.00 ± 0.19 , 8, 4, $p = 0.1934$, VIP INs, 0.73 ± 0.22 , 12, 6, $*p = 0.0151$; POm input, PV INs, 1.29 ± 0.27 , 10, 4, $p = 0.9219$, SST INs, 0.18 ± 0.05 , 16, 8, $****p < 0.0001$, nonVIP-5HT3aR INs, 1.09 ± 0.26 , 7, 5, $p = 0.6875$, VIP INs, 1.11 ± 0.36 , 13, 4, $p = 0.0942$; Ect/PRh input, PV INs, 1.46 ± 0.36 , 9, 5, $p = 0.4961$, SST INs, 0.47 ± 0.23 , 11, 6, $*p = 0.0420$, nonVIP-5HT3aR INs, 2.28 ± 0.64 , 4, 3, $p = 0.2500$, VIP INs, 1.27 ± 0.42 , 7, 3, $p = 0.9375$). Wilcoxon signed-rank test.

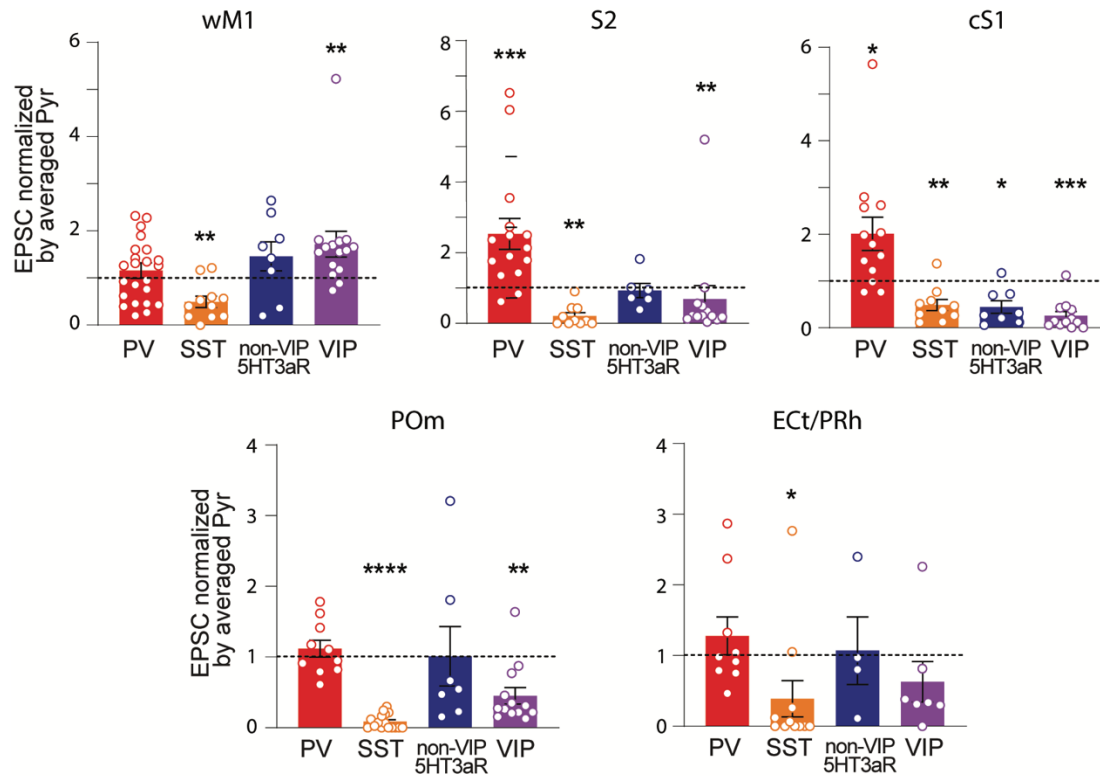


Figure S3. Long-range inputs from diverse brain areas to the different types of GABAergic interneurons in the supragranular layers of S1. Related to Figure 2. Population data showing Photostimulation-evoked EPSCs of individual GABAergic INs were normalized to the averaged EPSCs recorded from all pyramidal neurons in the same animal (Input area, type of GABAergic IN, mean \pm s.e.m., number of recorded neurons, number of mice used, p value; wM1 input, PV INs, 1.15 ± 0.16 , 23 from 6 mice, $p = 0.2861$, SST INs, 0.49 ± 0.11 , 11 from 4 mice, $**p = 0.0098$, nonVIP-5HT3aR INs, 1.45 ± 0.3 , 8 from 3 mice, $p = 0.25$, VIP INs, 1.59 ± 0.27 , 15 from 7 mice, $**p = 0.0043$; S2 input, PV INs, 2.53 ± 0.43 , 15 from 6 mice, $***p = 0.0006$, SST INs, 0.21 ± 0.09 , 10 from 5 mice, $**p = 0.002$, nonVIP-5HT3aR INs, 0.93 ± 0.2 , 6 from 2 mice, $p = 0.4375$, VIP INs, 0.68 ± 0.38 , 13 from 5 mice; cS1 input, PV INs, 2.01 ± 0.35 , 13 from 5 mice, $*p = 0.0105$, SST INs, 0.48 ± 0.11 , 10 from 6 mice, $**p = 0.0059$, nonVIP-5HT3aR INs, 0.44 ± 0.13 , 8 from 4 mice, $*p = 0.0156$, VIP INs, 0.25 ± 0.09 , 12 from 6 mice, $***p = 0.001$; POm input, PV INs, 1.11 ± 0.12 , 10 from 4 mice, $p = 0.5566$, SST INs, 0.08 ± 0.02 , 16 from 8 mice, $****p < 0.0001$, nonVIP-5HT3aR INs, 1.01 ± 0.42 , 7 from 5 mice, $p = 0.375$, VIP INs, 0.45 ± 0.11 , 13 from 4 mice, $**p = 0.0017$; Ect/PRh input, PV INs, 1.27 ± 0.26 , 9 from 5 mice, $p = 0.8203$, SST INs, 0.38 ± 0.25 , 11 from 6 mice, $*p = 0.04$, nonVIP-5HT3aR INs, 1.07 ± 0.47 , 4 from 3 mice, $p = 0.625$, VIP INs, 0.62 ± 0.28 , 7 from 3 mice, $p = 0.2188$). Wilcoxon signed-rank test, $*p < 0.05$, $**p < 0.005$, $***p < 0.0005$.

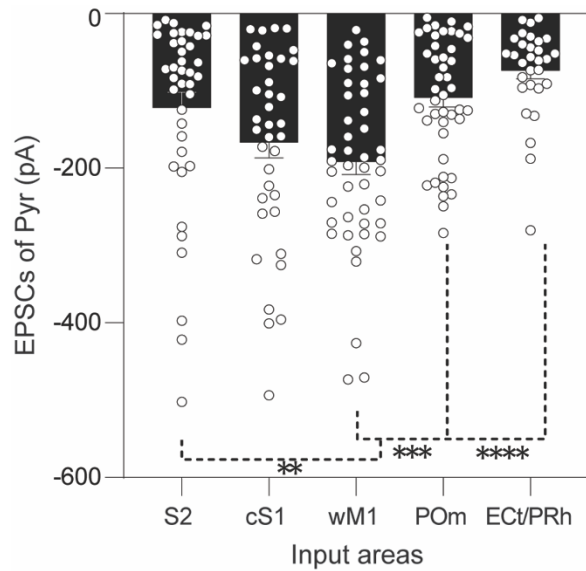


Figure S4. Long-range excitatory inputs from diverse brain areas to pyramidal neurons in the supragranular layers of S1. Related to Figure 2. The peak amplitude of photostimulation-evoked EPSC from each pyramidal cell was compared among different input areas (mean \pm s.e.m., S2 input, -121.53 ± 19.63 , $n = 39$, 18 mice; cS1 input, -166.64 ± 20.08 , $n = 38$, 21 mice; wM1 input, -191.78 ± 16.28 , $n = 46$, 20 mice; POm input, -108.99 ± 11.82 , $n = 44$, 21 mice; ECt/PRh input, -73.69 ± 10.68 , $n = 30$, 17 mice). One-Way ANOVA followed by the Holm Sidak's multiple comparisons test; ** $p = 0.0041$ for wM1 vs. S2, *** $p = 0.0006$ for wM1 vs. POm, **** $p < 0.0001$ for wM1 vs. ECt/PRh, *** $p = 0.0009$ for ECt/PRh vs. cS1.

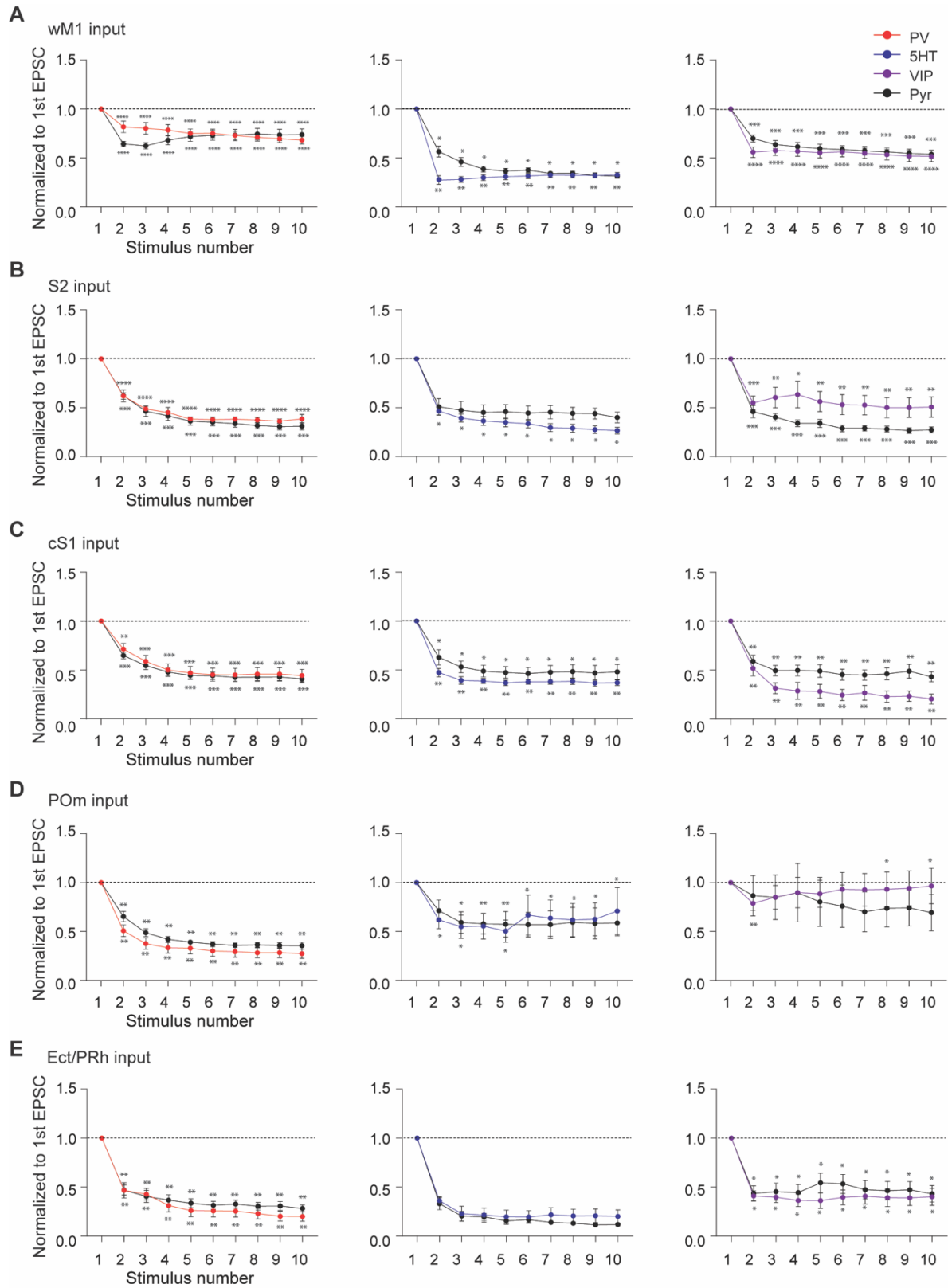


Figure S5. Synaptic depression of long-range excitatory inputs to different types of neurons in the supragranular layers of S1. Related to Figure 4. A train of 10Hz photostimulation-evoked depressing EPSCs were recorded from PV INs, nonVIP-5HT3aR INs, VIP INs and Pyr cells, regardless of long-range input areas. Normalized EPSCs were plotted against stimulus number. For each neuron, peak amplitude of EPSCs were normalized to that of 1st EPSC in a train of 10Hz photostimulation (wM1 input, PV INs (n=23), nonVIP-5HT3aR INs (n=8), VIP INs (n=15); S2 input, PV INs (n=15), nonVIP-5HT3aR (n=6), VIP INs (n=13); cS1 input, PV INs (n=13), nonVIP-5HT3aR INs (n=8), VIP INs (n=12); POm inputs, PV INs (n=10), nonVIP-5HT3aR (n=7), VIP INs (n=13); ECt/Prh inputs, PV INs (n=9), nonVIP-5HT3aR (n=4), VIP INs (n=7)). Wilcoxon signed-rank test; **** $p < 0.0001$, *** $p < 0.0005$, ** $p = 0.005$, * $p < 0.05$.

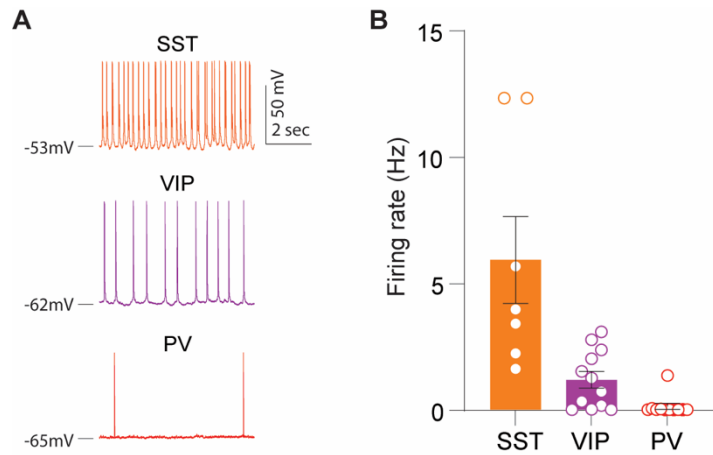


Figure S6. Spontaneous firing rates of different types of GABAergic neurons in modified ACSF. Related to Figure 6. Example traces (**A**) and population data (**B**) of spontaneous activity of SST INs, VIP INs and PV INs in the supragranular layers of S1. Under bath perfusion of a modified ACSF solution (see Methods), spontaneous activity of SST INs was significantly increased compared to those of VIP INs and PV INs. Spontaneous activity was recorded at the resting membrane potential (V_{rest}) indicated next to the voltage traces. SST INs, 5.92 ± 1.71 Hz, $n=7$, 3 mice; VIP INs, 1.18 ± 0.33 Hz, $n=12$, 3 mice; PV INs, 0.13 ± 0.12 Hz, $n=11$, 3 mice.

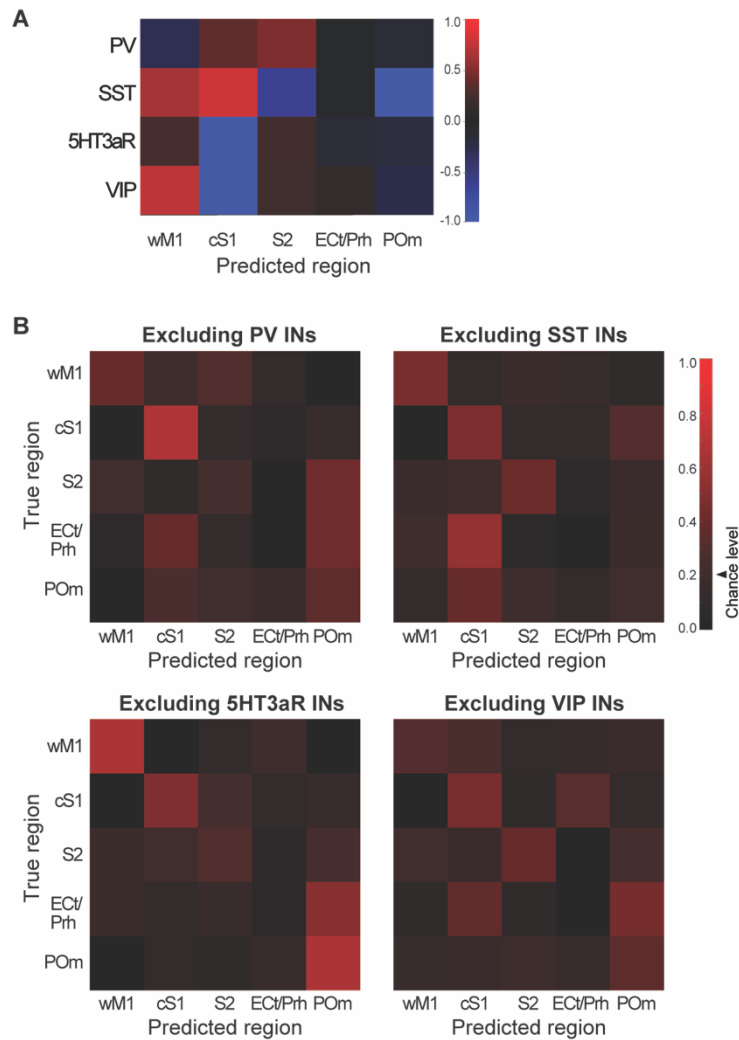


Figure S7. Long-range input area provides a distinct pattern of differential synaptic weights onto different GABAergic IN types. Related to Figure 7. (A) Weights of multinomial regression classifier for each type of GABAergic INs to five input areas. (B) Confusion matrices excluding each GABAergic IN subtype from training multinomial regression classifier.